SINTEF
PROCEEDINGS
2

Proceedings of the 12th International Conference on Computational Fluid Dynamics in the Oil & Gas, Metallurgical and Process Industries

Progress in Applied CFD – CFD2017

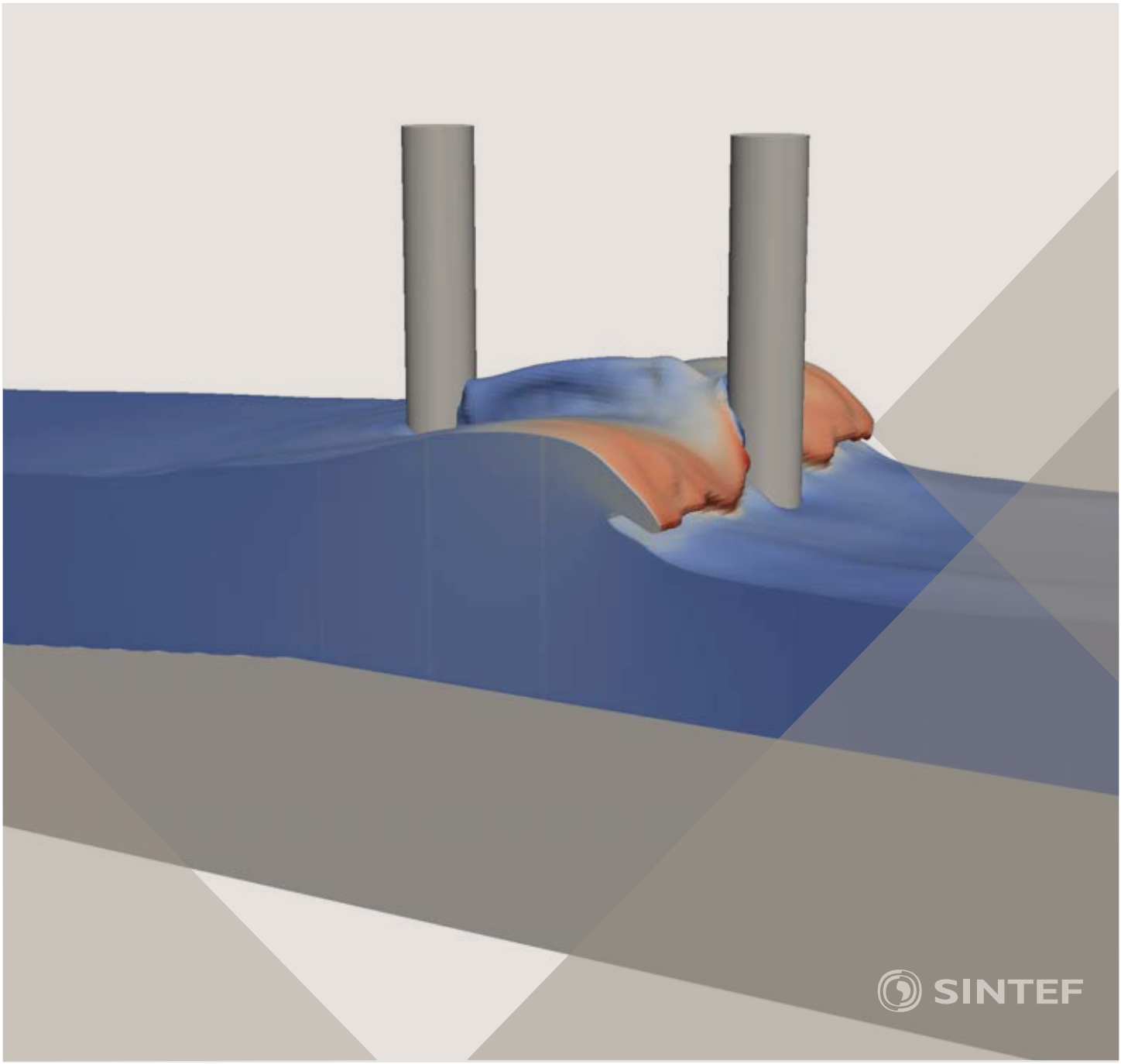

SINTEF Proceedings

Editors:
Jan Erik Olsen and Stein Tore Johansen

Progress in Applied CFD – CFD2017

Proceedings of the 12th International Conference on Computational Fluid Dynamics in the Oil & Gas, Metallurgical and Process Industries

SINTEF Academic Press

SINTEF Proceedings no 2
Editors: Jan Erik Olsen and Stein Tore Johansen
Progress in Applied CFD – CFD2017
Selected papers from 10th International Conference on Computational Fluid Dynamics in the Oil & Gas, Metallurgical and Process Industries

Key words:
CFD, Flow, Modelling

Cover, illustration: Arun Kamath

ISSN 2387-4295 (online)
ISBN 978-82-536-1544-8 (pdf)

SINTEF Academic Press
Address: Forskningsveien 3 B
PO Box 124 Blindern
N-0314 OSLO
Tel: +47 73 59 30 00
Fax: +47 22 96 55 08

www.sintef.no/byggforsk
www.sintefbok.no

SINTEF Proceedings
SINTEF Proceedings is a serial publication for peer-reviewed conference proceedings on a variety of scientific topics.
The processes of peer-reviewing of papers published in SINTEF Proceedings are administered by the conference organizers and proceedings editors. Detailed procedures will vary according to custom and practice in each scientific community.

PREFACE

This book contains all manuscripts approved by the reviewers and the organizing committee of the 12th International Conference on Computational Fluid Dynamics in the Oil & Gas, Metallurgical and Process Industries. The conference was hosted by SINTEF in Trondheim in May/June 2017 and is also known as CFD2017 for short. The conference series was initiated by CSIRO and Phil Schwarz in 1997. So far the conference has been alternating between CSIRO in Melbourne and SINTEF in Trondheim. The conferences focuses on the application of CFD in the oil and gas industries, metal production, mineral processing, power generation, chemicals and other process industries. In addition pragmatic modelling concepts and bio-mechanical applications have become an important part of the conference. The papers in this book demonstrate the current progress in applied CFD.

The conference papers undergo a review process involving two experts. Only papers accepted by the reviewers are included in the proceedings. 108 contributions were presented at the conference together with six keynote presentations. A majority of these contributions are presented by their manuscript in this collection (a few were granted to present without an accompanying manuscript).

The organizing committee would like to thank everyone who has helped with review of manuscripts, all those who helped to promote the conference and all authors who have submitted scientific contributions. We are also grateful for the support from the conference sponsors: ANSYS, SFI Metal Production and NanoSim.

Stein Tore Johansen & Jan Erik Olsen

Organizing committee:

Conference chairman: Prof. Stein Tore Johansen
Conference coordinator: Dr. Jan Erik Olsen
Dr. Bernhard Müller
Dr.Sigrid Karstad Dahl
Dr.Shahriar Amini
Dr.Ernst Meese
Dr.Josip Zoric
Dr.Jannike Solsvik
Dr.Peter Witt

Scientific committee:

Stein Tore Johansen, SINTEF/NTNU
Bernhard Müller, NTNU
Phil Schwarz, CSIRO
Akio Tomiyama, Kobe University
Hans Kuipers, Eindhoven University of Technology
Jinghai Li, Chinese Academy of Science
Markus Braun, Ansys
Simon Lo, CD-adapco
Patrick Segers, Universiteit Gent
Jiyuan Tu, RMIT
Jos Derksen, University of Aberdeen
Dmitry Eskin, Schlumberger-Doll Research
Pär Jönsson, KTH
Stefan Pirker, Johannes Kepler University
Josip Zoric, SINTEF

CONTENTS

MODELLING AND NUMERICAL SIMULATION OF SURFACE ACTIVE SPECIES TRANSPORT - REACTION IN WELDING PROCESSES

Kateryna DOROGAN

Industrial Risk Management Department, EDF R&D, 78401 Chatou Cedex, FRANCE

E-mail: kateryna.dorogan@edf.fr

ABSTRACT

This paper deals with the modelling of steel melting process during TIG welding operations on the nuclear power plants. The issue of the quality assurance of welding operations on some components is of great importance for the nuclear safety management. However, there are many parameters involved in the process which makes the uncertainty of the whole operation important. Moreover, some repair operations make impossible the quality control of the final weld bead. This is the case of one such a weld this study focus on. A way to ensure the quality of such weld beads could be based on the weld pool shape prediction by the numerical simulation. Thus, giving the operating parameters such as arc energy distribution, the flow simulation inside the weld pool could provide the information on the final weld pool dimensions.

The model describing the metal flow during the welding process developed in this work is based on the classical MHD and the enthalpy equations. Yet, the flow in the weld pool is mainly governed by variable surface tension force, the phenomenon known as Marangoni effect. The surface tension variation is in this case highly dependent on the thermal and the surfactant concentration gradients. In order to better evaluate this force, in this work, we present a new formulation of transport-reaction equations for surfactant and relative species in the molten steel. Moreover, this model takes into account species chemical reaction and evaporation. This allows mass fractions and gradients computation at the weld pool surface, and by this mean a better prediction of the surface tension force in case of variable chemical composition. The results of the simulations are compared to experimental data on the weld pool dimensions.

Keywords: Surfactants and interface, CFD, Free surface flow, MHD, Casting and solidification .

NOMENCLATURE

Greek Symbols

β	Thermal expantion coefficient, $[1/K]$
Γ_s	Excess of S concentration in solute, $[kg \cdot mol/m^2]$
γ	Surface tension force, $[N/m]$
γ_m^0	Surface tension of a pure metal at T_f, $[N/m]$
ε	Emissivity of the weld pool surface, $[1]$
η	Yield of the TIG process, $[1]$
λ	Thermal conductivity, $[W/m \cdot K]$
μ	Dynamic viscosity, $[kg/ms]$
μ_0	Vacuum permeability, $[V \cdot s/A \cdot m]$
ρ	Mass density, $[kg/m^3]$
ρ_{ref}	Density of the steel at the liquidus temperature, $[kg/m^3]$
σ	Electrical conductivity, $[Ohm \cdot m]$
σ_{SB}	Stefan-Boltzmann constant, $[W/m^2 \cdot K^4]$

Latin Symbols

$\mathbf{A}$	Magnetic potential, $[V \cdot s/m]$
$\tilde{A}$	Thermal surface tension gradient for a pure material, $[N/(m \cdot K)]$
a_s	Sulfur activity, $[1]$
$\mathbf{B}$	Magnetic field, $[T]$
C_p	Specific heat, $[J/K]$
$\mathbf{c}$	Vector of mass concentrations, $[kg/m^3]$
c_s	Sulfur mass concentration, $[kg/m^3]$
$\mathbf{D}_j^i$	Diffusion coefficient of species i in solute j, $[m^2/s]$
D_0^i	Frequency factor for species i, $[m^2/s]$
$\mathbf{E}$	Electric field, $[V]$
$\mathbf{F}_b$	Buoyancy, $[Pa/m]$
f_l	Liquid fraction, $[1]$
$\mathbf{g}$	Gravity, $[m/s^2]$
H	Total enthalpy, $[J]$.
ΔH	Heat of adsorption, $[J/(kg \cdot mol)]$
ΔH_s^{Cr}	Partial molar enthalpy of Cr-S interaction, $[J]$
h	Specific enthalpy, $[J/kg]$
$\tilde{h}$	Convective exchange coefficient, $[W/m^2 \cdot K]$
I	Current intensity, $[A]$
$\mathbf{j}$	Current density, $[A/m^2]$
$\mathbf{k}$	Segregation entropy factor, $[1]$
$\mathbf{n}$	Outward nomal vector, $[m]$
P_R	Electric potential, $[V]$
p	Pressure, $[Pa]$
Q^i	Activation energy for i-species, $[J/mol]$
R	Gas constant, $[J/mol \cdot K]$
r	Distance from heat source, $[m]$
r_H	Heat source dispersion, $[m]$
r_J	Current source dispersion, $[m]$
$\mathbf{S}_R^u$	Carman-Kozeny term, $[Pa/m]$
T	Temperature, $[K]$
T_f	Melting point, $[K]$
T_l	Liquidus temperature, $[K]$
T_{ref}	Reference temperature, $[K]$
T_s	Solidus temperature, $[K]$
T_0	Ambient temperature, $[K]$
t	time, $[s]$
U	Current tension, $[V]$
$\mathbf{u}$	Fluid velocity, $[m/s]$
$\mathbf{v}$	Welding torch speed, $[m/s]$

$\mathbf{x}$ Space coordinates vector, $[m]$
Y_i i-species mass fraction, $[1]$

Sub/superscripts
Cr Chromium
Fe Iron
Mn Manganese
S Sulfur

INTRODUCTION

This paper is aimed at proposing a new modelling of reacting metal flow formed in the weld pool during Tungsten Inert Gas (TIG) welding operations. Welding being one of the most used repair processes in nuclear engineering, the quality assessment of weld beads appears to be one of the important issues both from nuclear safety and industrial costs points of view. For instance, we are interested in reproducing numerically one such a weld found on French nuclear power plants. This weld appears to be difficult to control and reproduce experimentally due to local variations in chemical composition of welded materials. Moreover, the process make impossible the weld quality control upside down the pieces so that some internal defects could remain unrevealed. Till today, several experimental studies were made in order to understand and reproduce the most critical of those, but these attempts have been mostly unsuccessful.

An alternative approach to tackle this problem could be based on the weld pool shape predictions using numerical simulation tools. The model the most widely used to predict the flow pattern in the weld pool is based on the unsteady MHD equations taking into account the Marangoni effect which consists in modelling the surface tension force as a function of temperature and of surfactant concentration on the weld pool surface (Belton, 1976; Heiple and Roper, 1982; Sahoo *et al.*, 1988; McNallan and DebRoy, 1991; Mills *et al.*, 1998; Sampath and Zabaras, 2001).

However, these simulations were only successful in the case of constant chemical composition. In fact, in most practical situations, when two or more different materials are welded, the local variation of the surfactant content causes the modification of the flow characteristics, and an important difference on the weld pool shape may appear. This is for instance the case for sulfur which is known to modify the surface tension of the molten steel. It was found that the surface tension variation with the temperature is non monotonous and highly dependent on the sulfur concentration and its gradient. Moreover, the sulfur concentration in the liquid steel varies with the time and with the temperature since sulfur may create solid inclusions with manganese. Therefore, an accurate evaluation of species mass fractions in the unsteady metal flow is essential for the correct prediction of the surface tension force in these situations.

Thus, this paper presents the new transport-reaction equations of surfactant and relative species in the molten steel together with the MHD and the enthalpy equations describing the flow in the weld pool. It takes into account sulfur and manganese reversible chemical reaction and manganese evaporation.

WELD POOL MODEL DESCRIPTION

Geometry and Mesh

We deal with two fitted steel plates each of size $80 \times 40\ mm^2$ and of thickness $2\ mm$ put together, thus forming the whole domain of dimensions $80\ mm \times 80\ mm \times 2\ mm$, Fig. 1. In the figure, the red line shows the separation between pieces by the plane $y = 0$.

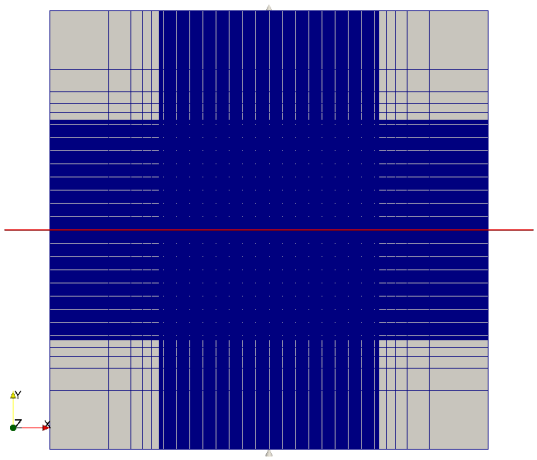

Figure 1: Geometry and mesh of the domain, 2d-cut.

The mesh shown in Fig. 1 is orthogonal and composed of 1.4×10^6 cells with the size of $1.25 \times 10^{-4}\ m$ in the finest central square region of size $40 \times 40\ mm^2$.

Magnetohydrodynamics equations

The model is a system of incompressible Navier-Stokes and Maxwell equations. For $\mathbf{x} \in R^3$, $t > 0$ and the state vector $(\mathbf{u}, p, h, P_R, \mathbf{A})^t(\mathbf{x}, t)$ we solve numerically :

Mass continuity equation :

$$\nabla(\rho\mathbf{u}) = 0, \tag{1}$$

Momentum conservation :

$$\frac{\partial(\rho\mathbf{u})}{\partial t} + \nabla(\rho\mathbf{u}\otimes\mathbf{u}) = -\nabla p + \mu\Delta\mathbf{u} + \mathbf{j}\times\mathbf{B} + \mathbf{F}_b + \mathbf{S}_R^u, \tag{2}$$

Specific enthalpy conservation :

$$\frac{\partial(\rho h)}{\partial t} + \nabla(\rho\mathbf{u}h) = \nabla\left(\frac{\lambda}{C_p}\nabla h\right) + \mathbf{j}\cdot\mathbf{E}, \tag{3}$$

Charge continuity equation :

$$\nabla(\sigma\nabla P_R) = 0, \tag{4}$$

Ampre's circuital law :

$$\Delta\mathbf{A} = -\mu_0\mathbf{j}, \tag{5}$$

with initial and boundary conditions detailed below. In (1)-(5), $\mathbf{u}$ denotes the fluid velocity, p the total pressure, h the specific enthalpy, P_R the real part of the scalar electric potential and $\mathbf{A}$ the vector magnetic potential. The thermodynamical properties of material are the density ρ, the dynamic viscosity μ, the specific heat C_p, the thermal conductivity λ and the electric conductivity σ, all varying as functions of the temperature (Kim, 1975).

The source terms in the momentum equation (2) correspond to the Laplace forces (expressed via the current density $\mathbf{j}$

and the magnetic field $\mathbf{B}$), the buoyancy $\mathbf{F}_b$ and the Carman-Kozeny term describing the velocity relaxation in the porous media during the liquid-solid transition $\mathbf{S}_R^u$ (Kozeny, 1927; Carman, 1956). The buoyancy is expressed using Boussinesq approximation:

$$\mathbf{F}_b = \rho_{ref}\,[1-\beta(T)(T-T_{ref})]\,\mathbf{g}, \tag{6}$$

with β the thermal expansion coefficient, T_{ref} the liquidus temperature of the steel, ρ_{ref} the density of the steel at T_{ref} and $\mathbf{g}$ the gravity. In the enthalpy conservation equation (3), the rhs term $\mathbf{j}\cdot\mathbf{E}$ represents the Joule effect, $\mathbf{E}$ denoting the electric field.
The form of equations (4), (5) is based on two assumptions: the fluid is supposed electrically neutral; the electric and magnetic fields are quasi stationary. Using the simplified Ohm's law: $\mathbf{j}=\sigma\mathbf{E}$, the system (1)-(5) is completed by the following relations:

$$\begin{aligned} \mathbf{E} &= -\nabla P_R, \\ \mathbf{B} &= \text{rot}\,\mathbf{A}. \end{aligned} \tag{7}$$

Initial conditions

We fix the initial difference of the electric potential between the electrodes $U = 11\ V$ as well as the current intensity $I = 135\ A$, thus giving the initial values to P_R and $\mathbf{A}$. At $t = 0$, we consider the workpiece in a solid state at ambient temperature $T_0 = 300\ K$, and atmospheric pressure, $p_0 = 101325\ Pa$. Then, the corresponding values of other properties for these values of pressure and temperature are : $\rho_0 = 7500\ kg/m^3$, $C_{p,0} = 602\ J\,K^{-1}\,kg^{-1}$ et $\mathbf{u}_0 = \mathbf{0}$.

Boundary conditions

The boundary conditions will be only detailed for the top (heated) surface of the plates. On the other boundary faces the default wall boundary conditions are fixed. Moreover, in practice there is no mass or momentum flux on these sides since they remain always in solid state.

- *Pressure*: $\partial P/\partial n = 0$.
- *Velocity*: We fix $\mathbf{u}.\mathbf{n} = 0$ and add a flux related to the weld pool surface tension variation, the surface tension $\gamma(\mathbf{c},T)$ being a function of the temperature T and of the chemical concentration of species composing the steel $\mathbf{c}$ (Belton, 1976):

$$\mu\frac{\partial \mathbf{u}}{\partial n} = f_l\cdot\sum_i \frac{\partial\gamma(\mathbf{c},T)}{\partial c_i}\cdot\nabla\, c_i + f_l\cdot\frac{\partial\gamma(\mathbf{c},T)}{\partial T}\cdot\nabla\, T. \tag{8}$$

with the liquid fraction f_l, defined as follows:

$$f_l = \begin{cases} 1, & T > T_l, \\ (T-T_s)/(T_l-T_s), & T_s \le T \le T_l, \\ 0, & T < T_s. \end{cases} \tag{9}$$

Among several surface active species which may be found in the steel during melting, sulfur is one that may be beforehand quantified since it is introduced in the steel during steel making process. It is also known to modify to a great extent the surface tension of binary Fe-S alloys (Heiple and Roper, 1982).

The most general expression of the surface tension force of the liquid metal containing surface active inclusions (for instance, sulfur) and varying with temperature is given by (Belton, 1976; Heiple and Roper, 1982; Sahoo *et al.*, 1988):

$$\gamma(c_s,T) = \gamma_m^0 - \tilde{A}(T-T_m) - RT\Gamma_s ln\,[1+Ka_s], \quad [N/m] \tag{10}$$

with

$$K = ke^{-\Delta H/RT}, \tag{11}$$

and with γ_m^0 the surface tension of a pure metal at T_f (with no inclusions), $\tilde{A}$ the opposite of $\partial\gamma(c_s,T)/\partial T$ for a pure material (without surface active inclusions), Γ_s the excess of sulfur concentration in solute, R the gas constant, k the segregation entropy, ΔH the heat of adsorption and a_s the sulfur activity.

Then, considering a more recent work (McNallan and DebRoy, 1991) which takes into account S-Cr interaction in liquid steel, the expression of the surface tension gradients induced by temperature and by sulfur concentration are written in the following form :

$$\begin{aligned} \frac{\partial\gamma(c_s,T)}{\partial T} &= -A - R\Gamma_s\left[\ln(1+Ka_s) + \frac{Ka_s}{1+Ka_s}\frac{\Delta H-\Delta H_s^{\text{Cr}}}{RT}\right], \\ \frac{\partial\gamma(c_s,T)}{\partial c_s} &= -\frac{RTK\Gamma_s}{1+Ka_s} \end{aligned} \tag{12}$$

with

$$a_s = 10^{e_s^{\text{Cr}}[pct\,Cr]}\cdot[pct\,S], \tag{13}$$

$$e_s^{\text{Cr}} = -94.2/T + 0.0396 \tag{14}$$

and with ΔH_s^{Cr} the partial molar enthalpy of Cr-S interaction in solute:

$$\Delta H_s^{\text{Cr}} = -94.2R[pct\,Cr]\ln 10. \tag{15}$$

Expression (8) describes the phenomenon known as the *Marangoni effect* which consists in the mass transfer along an interface between two fluids due to surface tension gradient. The latter is one of the most important forces acting in the weld pool.

- *Enthalpy*: The enthalpy flux fixed on the top surface is composed of the Gaussian-distributed heat source, radiative and convective heat exchange contributions moving with the torch speed in the x-direction:

$$\frac{\lambda}{C_p}\frac{\partial h}{\partial n} = \frac{\eta UI}{2\pi r_H^2}\exp\left(-\frac{r^2}{2r_H^2}\right) + \varepsilon\sigma_{SB}(T^4-T_0^4) + h(T-T_0), \tag{16}$$

with r_H the heat source dispersion, I the current intensity, U the current tension, η the yield of the process, $\sigma_{SB} = 5.67\times10^{-8}\ W\ m^{-2}\ K^{-4}$ the Stefan-Boltzmann constant, $\varepsilon = 0.5$ the emissivity of the weld pool surface, $T_0 = 300\ K$ the ambient temperature and $h = 15\ W\ m^{-2}\ K^{-1}$ the convective exchange coefficient.

- *Scalar electric potential and vector magnetic potential:*

$$\begin{aligned} \sigma\frac{\partial P_R}{\partial n} &= \frac{I}{2\pi r_J^2}\exp\left(-\frac{r^2}{2r_J^2}\right), \\ \frac{1}{\mu_0}\frac{\partial \mathbf{A}}{\partial n} &= 0. \end{aligned} \tag{17}$$

For the sake of simplicity, we assume the current source dispersion $r_J = r_H$.

Species transport-reaction equations

Since the surface tension gradients (12) are highly dependent on the sulfur concentration in the weld pool, it is essential to know the sulfur concentration at each time and position in the weld pool. Thus, in this section we detail the transport-reaction equations of the surface-active and related species. For instance, it is well known that Manganese addition is used in steel making processes to capture sulfur particles in order to prevent the steel from hot cracking during manufacturing. In fact, free-state sulfur atoms induce steel liquefaction by forming liquid inclusions with Fe:

$$Fe + S \rightarrow FeS \tag{18}$$

which are characterized by an extremely low melting point: $T_f(FeS) = 1261\ K$, thus reducing the melting point of the steel alloy. This may result in hot cracking defects.

To overcome this problem, desulfurization agents such as Manganese (Mn) are added in the steel during melting which allows the liquid inclusions FeS to be replaced by solid inclusions MnS with a higher melting point, $T_f(MnS) = 1893\ K$:

$$T_f(MnS) > T_f(FeS).$$

Therefore, in the present work, we are interested in modelling the following species-related phenomena:

- The sulfur content in the steel is limited to 0.03% weighted percent, and the Manganese content to 2%.
- **The chemical reaction** between sulfur in solute and Manganese to form MnS takes place during cooling at $T_{reac} = 1853\ K$:

$$FeS + Mn \rightarrow MnS + Fe. \tag{19}$$

  Since this reaction takes place at the temperature below the MnS melting point, it results in solid inclusions in liquid steel. These inclusions are created in the region with the appropriate temperature level and especially during the solidification.

- **Manganese evaporation** which takes place at temperatures $T > 2000K$ depending on the saturation pressure and boiling temperature (Pischke, 1994).
- **Diffusion coefficients of species** dependent on the chemical composition of the steel are rather difficult to determine at high temperatures. They are generally expressed as:

$$D^i_{304L}(T) = D^i_0 e^{(-Q^i/RT)} \quad [m^2/s], \tag{20}$$

  with D^i_0 the frequency factor and Q^i activation energy. Following some references (Potard, 1972; Chybanova, 2000), we found the following expressions of these coefficients for sulfur and Manganese:

$$\begin{aligned} D^S_0 &= 2.33 \times 10^{-7}\ m^2/s \quad \text{et} \quad Q^S = 52200\ J/mol, \\ D^{Mn}_0 &= 3.85 \times 10^{-7}\ m^2/s \quad \text{et} \quad Q^{Mn} = 69500\ J/mol. \end{aligned} \tag{21}$$

- **Thermophoresis (Soret effect)**. Considering Lewis number which gives the rate of the thermal diffusion to the mass diffusion is high enough, $Le(T) \approx 10^2$ as well as Prandtl number which gives the rate of the momentum diffusivity to the thermal diffusivity, $Pr(T) \approx 0.05$, it seems that the thermophoresis is an important phenomenon to be taken into account. It mainly depends on the thermal gradient referred to the domain size. However, the definition of the thermo diffusion coefficient in the liquid metal seems quite complicated, since most often found expressions are based on gas theory and never for high temperature liquid (Talbot *et al.*, 1980; Alam *et al.*, 2009).

In generalized form, the transport-reaction equation of Y_i species (S, Mn) is written :

$$\begin{aligned} \partial_t(\rho Y_i) + \nabla(\rho \mathbf{u} Y_i) - \nabla\left(\rho \mathbf{D}^{Y_i}_{304L} \nabla Y_i\right) = \nabla\left[\left(\mathbf{D}^{Y_i}_{th} \frac{\nabla T}{T}\right) \rho Y_i\right] \\ - K(T) \rho Y_i Y_j + S^{Y_i}_{evap}, \ \text{ with } K = K_0 e^{\left(-\frac{E_a}{RT}\right)} \end{aligned} \tag{22}$$

with Y_i the i-species mass fraction, $Y_i \in [0,1]$, $\mathbf{D}^{Y_i}_{304L}$ the mass diffusion coefficient of the i-species in the alloy (20), $\mathbf{D}^{Y_i}_{th}$ the thermophoretic diffusion coefficient of the i-species, $K(T)$ the rate constant for a bimolecular phase reaction, $S^{Y_i}_{evap}$ evaporation source term involved in Mn equation only. Moreover, we note that the MnS chemical reaction takes place at $T = 1853\ K$. Then, the enthalpy equation in (1)-(5) is modified to take into account these contributions: the concentration gradients, the latent heat of evaporation and chemical reaction contribution (though, in this case MnS reaction is isothermal).

Equations (22) together with system (1)-(5), (7) with initial and boundary conditions described in the previous section allow a more physical modelling of the surface tension variations (8) in the case of important thermal and concentration gradients.

RESULTS

The simulations were performed with *Code_Saturne* open source CFD software developed by EDF (Archambeau *et al.*, 2004). It is devoted to unsteady single phase simulations with complex reactive physics, turbulence and scalar transport. It is mainly based on the pressure correction algorithm and uses the finite volume numerical schemes. For more detailed presentation, the reader is referred to the technical documentation available online, `http://code-saturne.org`.

Given the welding parameters :

- the initial difference of the electric potential $U = 11\ V$,
- the current intensity $I = 135\ A$,
- the welding torch speed $v = 16.3\ cm/min$,

as well as the geometry and the mesh described in "Geometry and Mesh" section (Fig. 1) with the cell size of $1.25 \times 10^{-4}\ m$ and the time step $\Delta t = 10^{-3}\ s$, we present here some results coming from weld pool simulations of a practical welding operation used as a validation test case. The pieces to be welded include a discontinuity of the chemical composition which corresponds for instance to an initial discontinuity in sulfur content as shown in Fig. 2, 3 with Low sulfur content of 0.0008 $wt\%$ (blue) and

High sulfur content of 0.005 *wt%* (red). In this example, High sulfur material represents the filler metal often used in welding operations to improve the weld pool penetration.

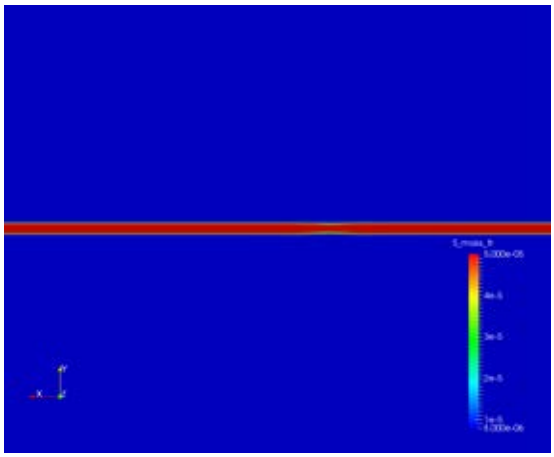

Figure 2: The sulfur mass fraction presenting a discontinuity (the filler metal) at t = 0 s, top surface view, $z = 0.002$.

Figure 3: The sulfur mass fraction presenting a discontinuity (the filler metal) at t = 0 s, $x = 0$ cut.

The results presented in Fig.4 - Fig.9 show the velocity, pressure, temperature and surface tension gradient wrt the temperature approximations as well as the spatial distribution of the sulfur mass fraction in the weld pool at the stationary state. We can see that the negative values of the surface tension gradient wrt the temperature imply the outward fluid velocities on the top surface which result in more spreading weld pool.

We've also performed a sensitivity analysis of the results on the mean sulfur content in the weld pool. It appeared that the external weld pool width is decreasing with a growing sulfur concentration and that at the same time, the internal width is increasing for the sulfur content above 0.006 *wt%*. This is a quite relevant conclusion which reflects the correct treatment of the surface tension variation with sulfur content. In fact, the surface tension force on the weld pool surface is known to decrease with an increasing sulfur concentration. Moreover, the surface tension gradient wrt the temperature changes the sign when the sulfur concentration exceeds 0.005 *wt%*. Thus, the flow direction in the weld pool turns opposite : we expect to have a more penetrating weld pool for high sulfur concentration versus a more spreading one for low sulfur content (Heiple and Roper, 1982; McNallan and DebRoy, 1991).

Then, Figures 10 and 11 show the final weld pool shape in a stationary state whose dimensions (external and internal widths) are highly dependent on the initial sulfur content. We compare these dimensions with the experimental data provided by operating company for a welding operation performed in the same operating conditions. We note that

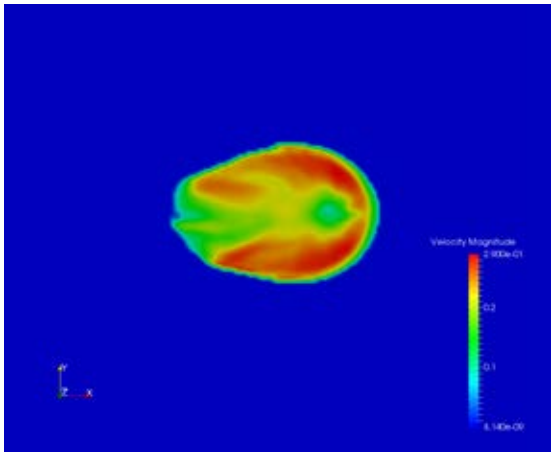

Figure 4: The fluid velocity in the stationary regime, top surface view with $z = 0.002$.

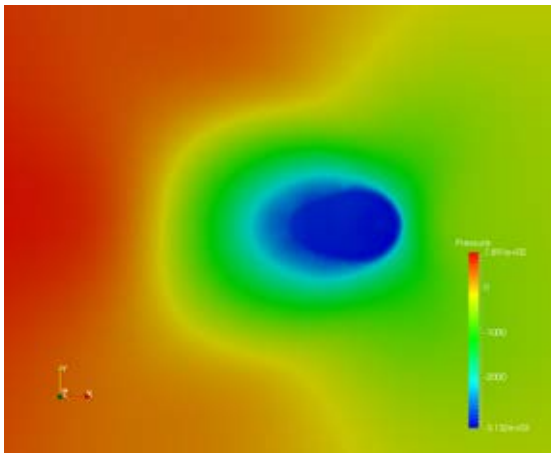

Figure 5: The pressure approximation in the stationary regime, top surface view with $z = 0.002$.

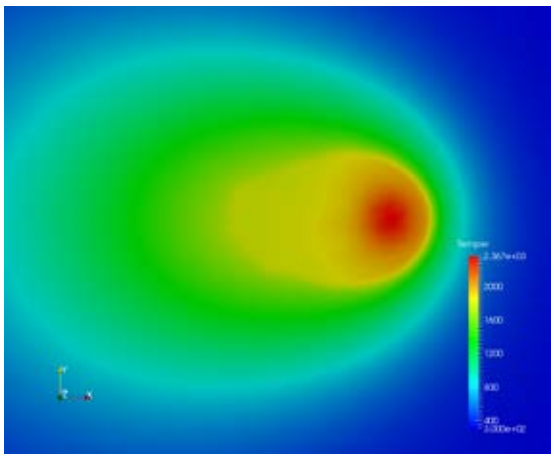

Figure 6: The temperature approximation in the stationary regime, top surface view with $z = 0.002$.

the data on the weld pool dimensions obtained in this case are in quite good agreement (Table1).

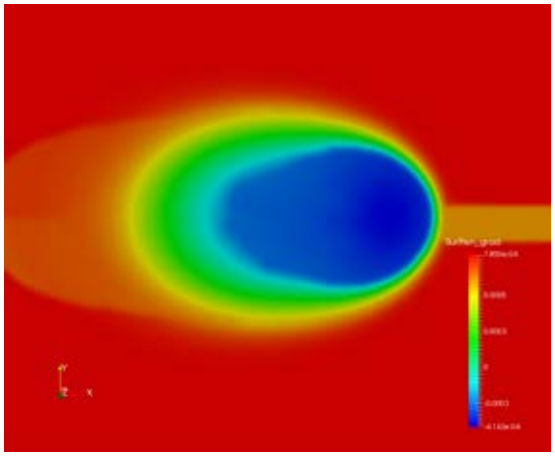

Figure 7: The surface tension gradient induced by temperature in the stationary regime, top surface view with $z = 0.002$.

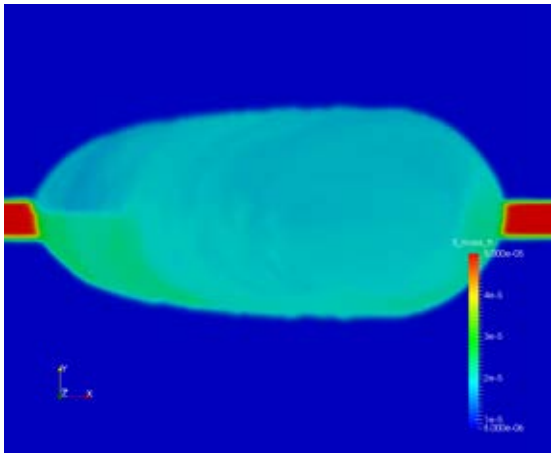

Figure 8: The sulfur mass fraction in the stationary regime, top surface view with $z = 0.002$.

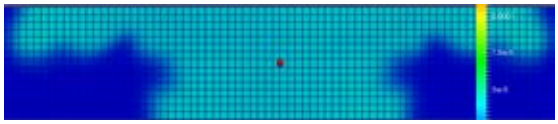

Figure 9: The sulfur mass fraction in the stationary regime, $x = 0.005$ cut.

Table 1: Comparison of weld pool dimensions

	Simulation	Measurement
External width (mm)	8.4	8.2
Internal width (mm)	4.26	4.5

CONCLUSION

Based on a practical case of a welding operation, we have introduced in this paper a new transport - reaction equations for surface active and related species which are involved in the surface tension modelling when studying welding and metal melting processes. This modelling is new and offers a tool for the unsteady quantification of the sulfur content in the molten steel all along the welding operation and the solidification. It takes into account sulfur and manganese chemical reaction, temperature dependent mass diffusion, manganese evaporation and thermophoresis. Moreover, the surface tension law accounts for sulfur and chromium interaction, which influences the sulfur surface activity. Some sensitivity analysis has also been made to study the global effect of the sulfur content on the weld pool dimensions. The numerical results obtained with these simulations are in good agreement with the experimental data, the conclusion which allows to validate both the modelling and the numerical approach for the present case.

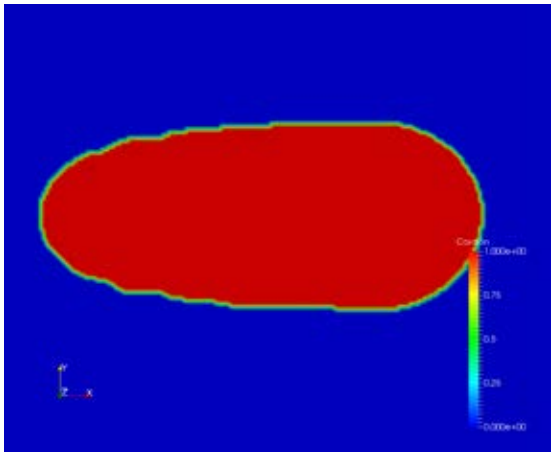

Figure 10: Final weld bead shape, top surface view with $z = 0.002$.

Figure 11: Final weld bead shape, $x = 0.005$ cut.

REFERENCES

ALAM, M., RAHMAN, M. and SATTAR, M. (2009). "Transient magnetohydrodynamic free convective heat and mass transfer flow with thermophoresis past a radiate inclined permeable plate in the presence of variable chemical reaction and temperature dependent viscosity". *Nonlinear Analysis: Modelling and Control*, **14(1)**, 3–20.

ARCHAMBEAU, F., MECHITOUA, N. and SAKIZ, M. (2004). "Code_saturne: a finite volume code for the computation of turbulent incompressible flows". *Int. J. Finite Volumes*, **1**, 1–62.

BELTON, G. (1976). *Metall.Trans. B*, **7B**, 35–42.

CARMAN, P. (1956). *Flow of gases through porous media*. Butterworths, london ed.

CHYBANOVA, L. (2000). *Proprietes physico-chimiques des metaux liquides contenants des sulfures et des oxydes et la cinetique des echanges a la limite avec les materiaux de construction*. Ph.D. thesis, Oural Technical Uniersity.

HEIPLE, C. and ROPER, R. (1982). "Mechanism for minor element effect on gta fusion zone geometry". *Weld. J.*, **61(4)**.

KIM, C.S. (1975). "Thermophysical properties of stainless steels". *Argonne National Laboratory*.

KOZENY, J. (1927). "Ueber kapillare leitung des wassers im boden". *Sitzungsber Akad. Wiss., Wien*, **136(2a)**, 271–306.

MCNALLAN, M. and DEBROY, T. (1991). "Effect of temperature and composition on surface tension in fe-ni-cr

alloys containing sulfur". *Metallurgical Transactions*, **22B**, 551–560.

MILLS, K., KEENE, B., BROOKS, R. and SHIRALI, A. (1998). "Marangoni effects in welding". *Phil. Trans. R. Soc. Lond.*, **356**, 911–925.

POTARD, C. (1972). *Contribution a l'etude de la diffusion dans les alliages liquides ternaires. Application a la solidification.* Ph.D. thesis, Grenoble.

SAHOO, P., DEBROY, T. and MCNALLAN, M.J. (1988). "Surface tension of binary metals - surface active solute systems under conditions relevant to welding metallurgy". *Metallurgical Transactions*, **19B(483)**.

SAMPATH, R. and ZABARAS, N. (2001). "Numerical study of convection in the directional solidification of a binary alloy driven by the combined action of buoyancy, surface tension, and electromagnetic forces". *Journal of Computational Physics*, **168**, 384–411.

TALBOT, L., CHENG, R., SCHEFER, A. and WILLS, D. (1980). "Thermophoresis of particles in a heated boundary layer". *J. Fluid Mech.*, **101**, 737–758.